ARTICLE

Three-Dimensional Control of Self-Assembled Quantum Dot Configurations

Michael K. Yakes, Cory D. Cress, Joseph G. Tischler, and Allan S. Bracker*

Naval Research Laboratory, 4555 Overlook Avenue SW, Washington, D.C. 20375

ABSTRACT We demonstrate techniques for growing three-dimensional quantum dot configurations using molecular beam epitaxy on faceted template islands. Molecular beam shadowing leads to new geometries through selective nucleation of the dots on the template edges. Strain-induced stacking converts the planar configurations into three-dimensional structures. The resulting dot morphologies and their configurational uniformity are studied using cross sectional scanning tunneling microscopy and atomic force microscopy. Combining photoluminescence measurements with structural characterization allows interpretation of the ensemble photoluminescence spectrum. Bright spectra for the three-dimensional structures suggest an improved method for combining lithographic nucleation sites with self-assembled dot growth. These techniques can be applied to lithographic templates to fabricate complex quantum dot networks.

KEYWORDS: quantum dot · photoluminescence · nucleation · droplet epitaxy · molecular beam epitaxy

To take full advantage of the potential of self-assembled quantum dots (QDs), methods must be developed to arrange QDs in complex, ordered networks.[1] Applications such as quantum information require precise positioning of QDs and control of interdot interactions with electrical or optical techniques. To date, the most widely studied system of interacting self-assembled QDs is a vertically stacked quantum dot molecule (QDM).[2−5] However, this system is limited by its one-dimensional nature and is not easily scalable. Alternatively, a variety of techniques can been used to modify planar substrates to nucleate laterally coupled QDMs in two dimensions through molecular beam epitaxy.[6−14] Nanolithographic nucleation sites[15] appear to be the most versatile approach to growing QD structures with arbitrary complexity if significant challenges can be overcome. Only a small number of quantum dot geometries are possible on a single type of nucleation site, and the optical quality of the material is often degraded by imperfections that are introduced through lithographic processing.

In this work, we demonstrate general techniques to grow a variety of two- and three-dimensional QDMs on a simple nucleation site. These QDMs are configurationally uniform and the three-dimensional structures show greatly improved optical quality. As nucleation sites, we use homoepitaxial GaAs islands formed through droplet epitaxy.[14,16] To form these islands, gallium vapor is first deposited on a GaAs substrate in the absence of arsenic flux, forming gallium droplets. The gallium droplets are then crystallized upon exposure to arsenic.[17] Previous work has shown that InAs QDMs are nucleated on the GaAs islands in several configurations that can be controlled with the indium exposure.[18] In our work, lateral QDM geometries are selectively nucleated on particular facet edges of the template structure by controlling the substrate orientation with respect to the indium molecular beam source. The resulting QDMs are converted to three-dimensional configurations with bright optical spectra using strain-induced stacking. Atomic force microscopy (AFM) and cross sectional scanning tunneling microscopy (XSTM) are used to identify the morphology and uniformity of the grown structures. Low temperature photoluminescence measurements demonstrate the recovery of the optical properties in the three-dimensional configurations. Combining the structural characterization with the PL measurements allows assignment of features in the PL spectra.

RESULTS AND DISCUSSION

Structural Control of Lateral Quantum Dot Molecules. A schematic diagram and an atomic force microscopy (AFM) image of a GaAs island produced by droplet epitaxy

*Address correspondence to allan.bracker@nrl.navy.mil.

Received for review March 26, 2010 and accepted June 08, 2010.

Published online June 17, 2010. 10.1021/nn100623q

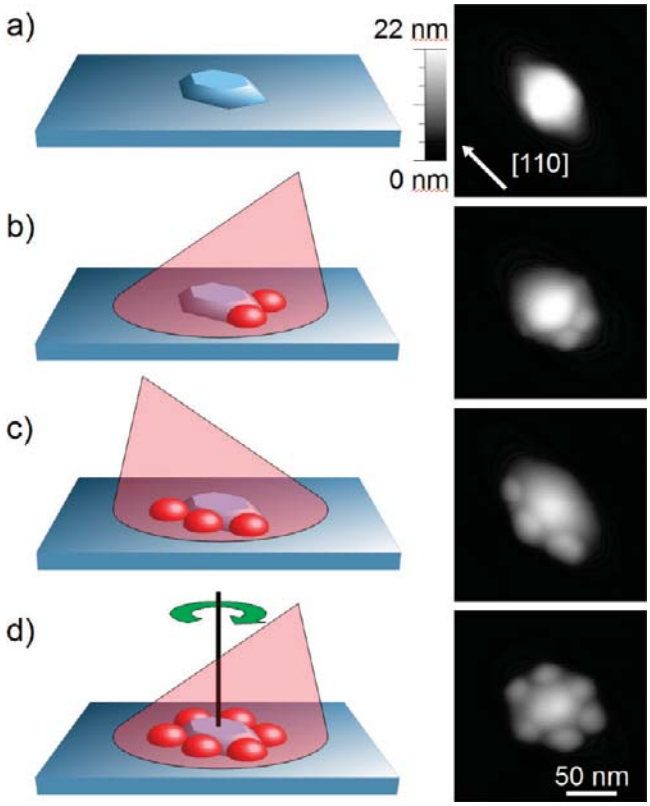

Figure 1. Geometry of QDMs controlled with incident angle of indium molecular beam: (a) schematic and AFM image of GaAs islands produced by droplet epitaxy; (b) bimolecule configuration resulting from indium beam flux oriented along the [110] direction; (c) trimolecule configuration resulting from beam flux along the [1$\bar{1}$0] direction; (d) hexamolecule configuration with sample rotated to average over the incoming In flux direction.

are shown in Figure 1a. The images of these structures from previous work have shown a hemispherical island shape;[14] however, the GaAs islands in Figure 1a show six facet edges, consistent with earlier observations of GaAs islands on AlGaAs.[19] The correlation of the faceted structure with the subsequent selective growth of up to six InAs QDs in the same angular arrangement suggests that the facets play an important role in nucleation of the QDs.

Figure 1b shows a GaAs island following exposure to indium flux along the [110] direction. Only the two edges that face the incoming indium beam nucleate QDs, forming a two dot QDM (bimolecule). This anisotropic configuration occurs even though the GaAs islands do not completely obscure the indium beam from the far side of the island that is facing away from the indium flux. With increasing InAs deposition along the [110] direction, additional QDs form on the faceted edges that are parallel to the indium beam direction, forming a quadmolecule (not shown). With further deposition, larger clusters of dots form on the near side of the island, but surprisingly, the shadowing effect is so prominent that dots do not form on the far side of the islands even when the InAs coverage is high enough to nucleate dots between the islands.

Changing the direction of the incoming indium flux creates new QDM configurations nucleated on different edges of the GaAs islands. When the indium beam flux is oriented along the [1$\bar{1}$0] direction, three edges of the GaAs island are exposed to the increased InAs flux and nucleate dots. This trimolecule configuration is shown in Figure 1c. Finally, if the sample is rotated during indium deposition all six edges of the island receive equal exposure and a symmetric hexamolecule configuration forms [Figure 1d].[14] Large scale AFM images show better than 80% of the GaAs islands nucleating a single QDM configuration for each of the configurations shown in Figure 1. These results demonstrate the high degree of control that can be obtained by manipulating the direction of the incoming indium beam.

Cross-sectional scanning tunneling microscopy (XSTM) is an ideal tool to study the morphology of capped QDMs, because it allows for atomic scale measurements of the buried structure with chemical sensitivity. Plan-view AFM cannot detect the interface between the materials, so it cannot resolve the vertical size of the InAs QDs independently of the underlying GaAs islands. Figure 2 shows images of InAs bimolecules grown with incident indium flux along the [110] direction. The sample was cleaved along the (110) and (1$\bar{1}$0) planes, exposing different features of the QDM. The images in Figure 2a show XSTM images of QDMs cleaved along the (110) plane, where two dots are visible. The InAs dots are the brightest regions of the image, while the InAs wetting layer appears as a less intense band. The first image shows a fairly symmetric bimolecule, and the next two are less symmetric. We believe that the fourth image (lower left) shows a cleave through the middle of a GaAs island, where smaller InAs QDs are grown on the island edges. The images in Figure 2b were cleaved along the (1$\bar{1}$0) plane, so only one dot is visible. Based on 18 separate molecules studied with XSTM we estimated the InAs dot dimensions independently of the buried GaAs island, yielding an average QD height of 8 nm and average center-to-center dot distance of 30 nm. These estimates are affected by the complicated QDM geometry and by the uncertainty in where the cleavage plane intersects the nanostructure but indicate that these QDMs are excellent candidates for studying electronic coupling effects.

Extending Lateral Quantum Dot Molecules into Three Dimensions. In general, it will be desirable to grow ordered QD networks in three dimensions, rather than just two. Here, we extend the lateral QDM configurations into three dimensions by taking advantage of the strain-induced nucleation technique that is often used to grow vertically coupled QD pairs.[20−22] This process is illustrated in Figure 3a. A first layer of QDMs is nucleated on GaAs islands in the usual way and then capped with GaAs. This produces a new growth surface with

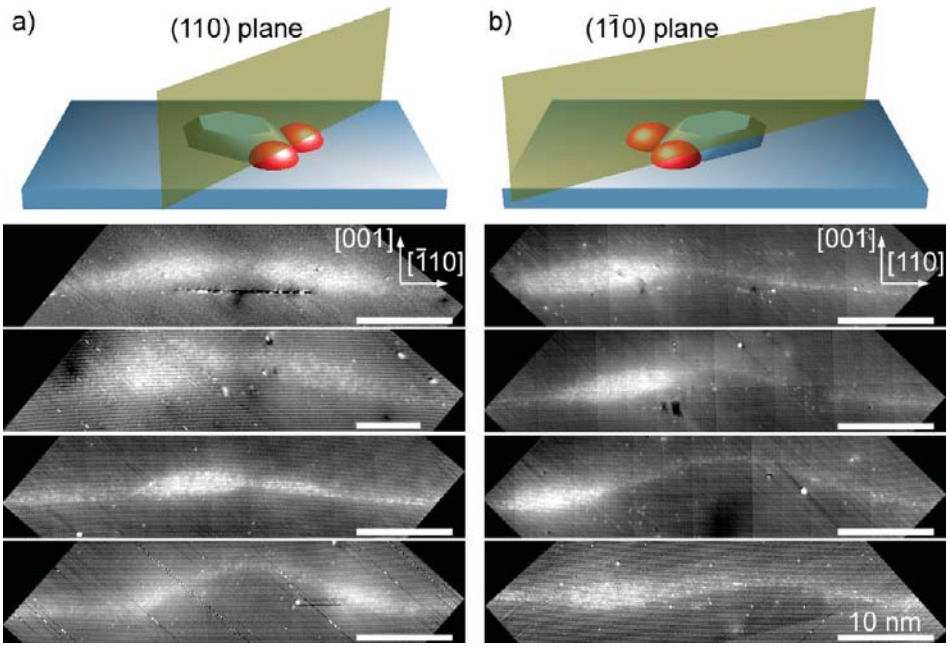

Figure 2. When the QDM is cleaved along (110) or (1$\bar{1}$0) planes, one or two dots in the QDM are exposed. (a) Filled state XSTM images cleaved along the (110) plane showing two dots (the bright regions in the center of the images). (b) Filled state XSTM images for samples cleaved along the (1$\bar{1}$0) plane showing a single dot.

broader and shallower GaAs islands that still protrude up from the first layer. When InAs dots are then grown on the capping layer, we find that they preferentially form above the buried InAs dots underneath.

Three samples were grown to investigate the role of strain-induced nucleation (Figure 3b–d) in lateral QDM formation. The growth of the first layer InAs dots was varied for each sample, but all were capped with 10 nm of GaAs, and the substrates were continuously rotated during growth of the second InAs QD layer. The AFM image in Figure 3b shows second layer QDMs grown above a nonrotated first layer with quadmolecules. Even though all sides of the island received equal flux during the second layer growth, dots only formed

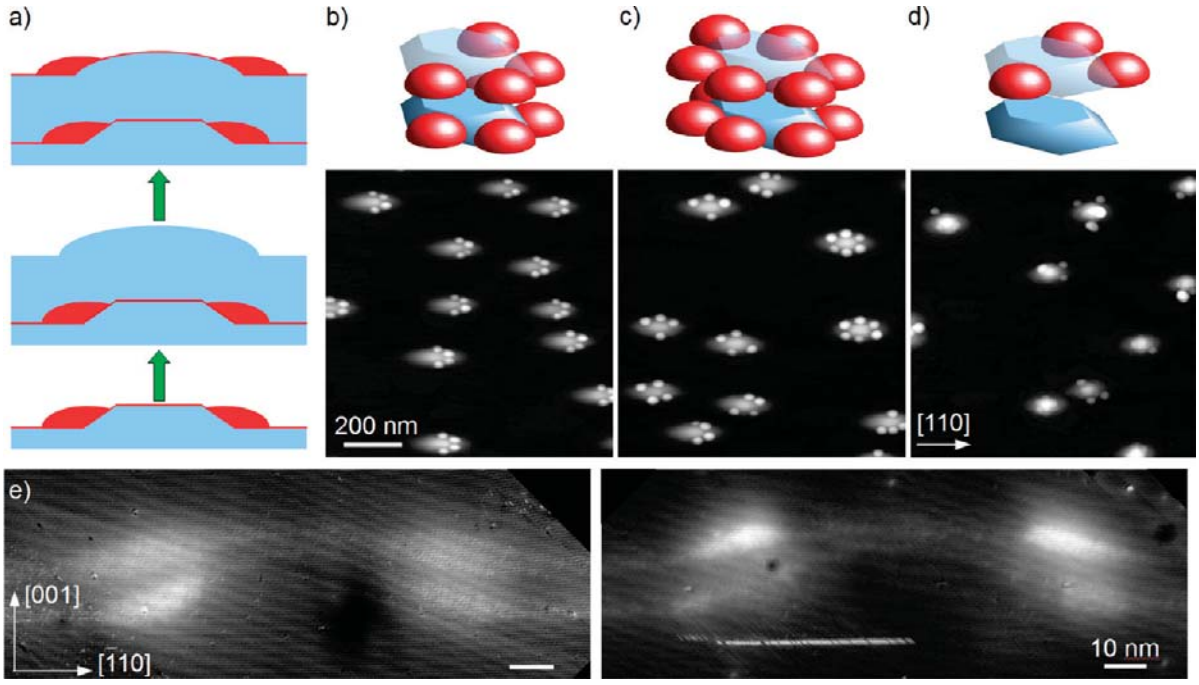

Figure 3. (a) Schematic diagram of the strain-induced nucleation technique for three-dimensional QDMs. Single layer QDMs are covered with 10 nm of GaAs. Second-layer InAs dots are grown while the substrate is rotated. (b–d) AFM images of QDs grown with (b) underlying quad-molecules, (c) underlying hexa-molecules, (d) no underlying dots. These results show that both strain-induced and island-induced nucleation play a role in the formation of second layer QDMs. (e) XSTM images cleaved along the (110) plane showing the stacked QDM.

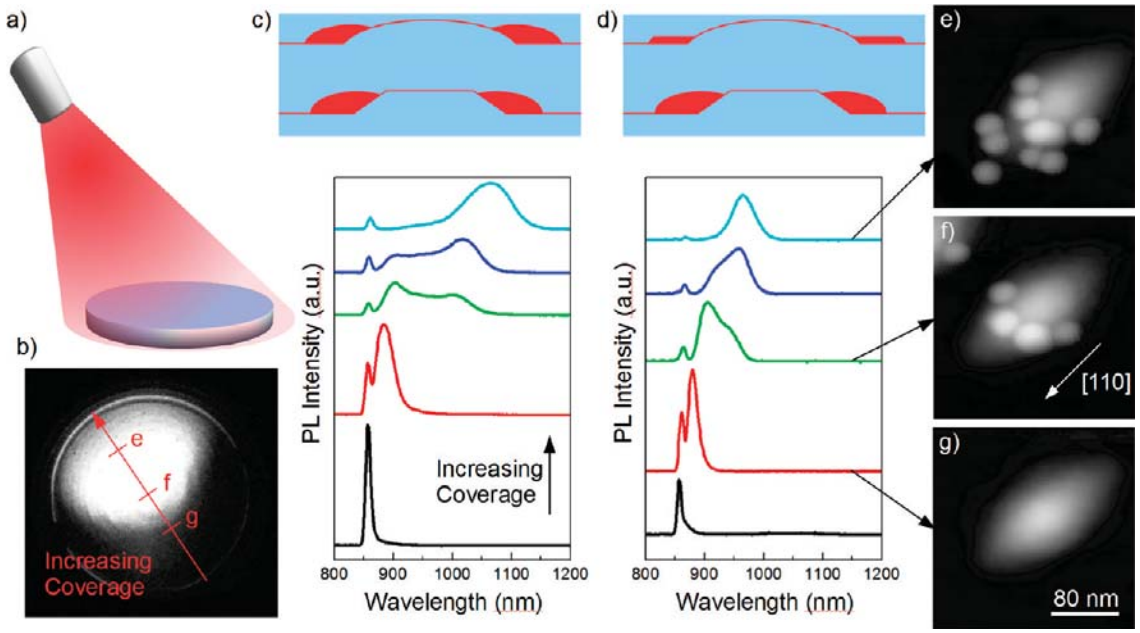

Figure 4. (a) Illustration of the wafer orientation during InAs dot growth. The indium beam flux direction determines the dot configuration while the flux gradient across the wafer determines the dot density. (b) PL wafer image showing the dot density gradient across the GaAs wafer. The image is taken using a long pass filter to emphasize the dot luminescence. (c−d) 10 K PL spectra of (c) 2 layer QDM structure and (d) 2 layer QDM structure where the second layer has been treated with a cap and flush procedure. (e−g) AFM images of structures used in PL measurements. Arrows indicate the approximate position of the corresponding PL spectra.

on the sides of the island where first layer dots are present underneath, demonstrating the importance of strain-induced nucleation. XSTM images in Figure 3e show two stacked molecules cleaved along the (110) plane. These images show that the GaAs cap above the first layer QDM is less than the nominal 10 nm capping distance. Figure 3c shows second-layer QDMs grown above a layer of hexamolecules produced with substrate rotation. In this case, second-layer dots appear all around the island. Some dots are missing in the second layer, possibly due to errors in the buried QDM template or insufficient InAs exposure to nucleate all six second-layer dots. When GaAs islands with no first layer InAs dots are capped, as in Figure 3d, second layer dots still nucleate around the remnant islands, although with lower probability and less geometric ordering than strain-induced nucleation. The nucleating effect of strain therefore appears to dominate that of the islands when both are present.

Identification of Ensemble Photoluminescence Features. We have grown a set of QDM samples to demonstrate the benefit of strain-induced stacking for photoluminescence (PL) intensity and to further investigate the ensemble PL spectrum. We have found that single layer QDMs grown with droplet epitaxy have a significantly reduced PL intensity compared with QDs grown on flat substrates. Stacked dots provide an approach to recover the PL intensity.[23] For PL measurements, the two QDM layers were separated by a barrier consisting of 5 nm of GaAs, 10 nm of $Al_{0.3}Ga_{0.7}As$, then an additional 5 nm of GaAs. The AlGaAs was included to further inhibit tunneling of carriers between the two layers of QDMs. These samples were not rotated during the growth of the second dot layer, allowing us to take advantage of the indium coverage gradient across the wafer to study the effect of coverage on the optical spectrum. The coverage gradient is due to the nonuniform flux from the indium source and is not necessarily parallel to the direction of the incoming indium beam as illustrated in Figure 4a. Three samples were grown under conditions that varied only in how the second layer QDMs were capped. In the first sample (Figure 4c), the second layer QDMs are capped at the growth temperature, which should produce dots with similar structure to those in Figure 2. In the second sample (Figure 4d) the height of the second layer QDMs was truncated by using the indium flush technique,[24,25] in which QDMs are partially capped with 2.8 nm of GaAs and then annealed. Finally, a third uncapped sample was grown for AFM measurements.

With samples for AFM and PL grown under nominally identical conditions, we can correlate features in the optical spectra to the QDM morphology. The spatial variation of the indium coverage across the wafer is easily determined by capturing a full wafer image of the low-temperature PL with an 895 nm long pass filter placed in front of a standard video camera (Figure 4b). In this arrangement, the PL from QDMs on the high-indium side of the sample appears brightly in the image, while the wetting layer PL on the low-indium side is blocked by the filter. From the image, we can directly observe the direction of the indium gradient and

measure PL spectra or AFM images at equivalent points along this gradient on all three samples.

Coverage-dependent series of PL spectra are shown for both the unflushed and flushed QDM samples in Figure 4 panels c and d, respectively. Both series show three distinct peaks. The peak near 870 nm corresponds to the InAs wetting layer and is most intense on the low-indium side of the sample, where no QDMs have formed. As the coverage increases, a second peak emerges out of the wetting layer. This peak redshifts to 900 nm as the coverage increases but disappears as a third peak appears at longer wavelengths. Interestingly, the second peak is most intense at a position on the wafer where the AFM sample still shows no QDM nucleation, shown in Figure 4g. The second peak is not affected by the indium flush, indicating that whatever structure is luminescing must have a vertical dimension less than the height of the GaAs partial cap (2.8 nm). We tentatively assign this peak to a thick wetting layer that forms at the edges of the GaAs islands prior to nucleation of QDMs. The third peak emerges at higher coverage and has a wavelength 1020−1080 nm for the unflushed sample and 950−980 nm for the flushed sample. It appears for a wafer position that corresponds to the appearance of QDMs on the AFM sample (Figure 4f). The third peak is therefore identified with the QDMs themselves.

The intensity of the PL in these spectra is comparable to spectra of InAs self-assembled QDs grown without the GaAs island template, demonstrating that the 20 nm GaAs/AlGaAs barrier between the layers is effective at inhibiting nonradiative recombination, while preserving ordered nucleation. Individual QDMs measured with microphotoluminescence also show comparable intensities to standard InAs dots.

CONCLUSION

We have demonstrated two molecular beam epitaxy techniques that can be used to grow a wide range of quantum dot geometries on a single type of nucleation site. Off-normal incidence of the molecular beams allows for growth of low-symmetry geometries, while strain-induced stacking adds structural complexity and the option of replicating an ordered geometry at a safe distance from lithographically processed surfaces. We anticipate that these techniques will translate well to purely lithographic nucleation templates, where there is wide flexibility to engineer the nucleation sites. The resulting hybrid of top-down and bottom-up techniques would provide a deterministic method to fabricate complex quantum dot networks.

METHODS

Sample Preparation and Growth. Samples were prepared on n-type GaAs wafers. A 200 nm GaAs buffer was grown at 600 C, then the sample was quenched to 400 C for Ga droplet deposition. Three monolayer equivalent of gallium was deposited with the arsenic cell closed, then the sample was cooled until the thermocouple read 100 C. The arsenic shutter was then opened and the gallium droplets recrystallized to islands by exposure to the arsenic beam for 90 s. The temperature was then ramped to 540 C and held for an additional 100 s. For QD growth the temperature was lowered to 500 C, and the indium source was opened for 54 s (60 s of indium exposure is required to form dots on flat substrates under similar conditions) under As beam equivalent pressure 5×10^{-7} Torr. The InAs source is oriented approximately 30 degrees away from the sample normal. For vertically stacked quantum dots GaAs and $Al_{0.3}Ga_{0.7}As$ buffer layers were deposited at 500 C. Samples for PL and XSTM were capped with 260−300 nm of p-doped GaAs, while AFM samples were left uncapped.

Cross-Sectional Scanning Tunneling Microscopy. To obtain an atomically abrupt cleave across the epilayer for XSTM measurements, the samples were thinned *ex situ* to <200 μm. After being loaded into the XSTM chamber (base pressure $<10^{-10}$ Torr), the samples were scribed and cleaved *in situ* to expose a (110) plane or ($1\bar{1}0$) plane perpendicular to the MBE growth direction. The constant-current 60−100 pA images shown here are of filled electronic states measured with sample bias of −3.0 V and a resolution of 1.0 or 1.5 Å/pixel.

Low-Temperature Ensemble Photoluminescence Spectroscopy. Photoluminescence spectra were measured from samples mounted in a coldfinger cryostat at 10 K. The samples were illuminated with 1 mW of 532 nm laser light focused to a spot diameter of 60 μm. The photoluminescence was dispersed with a double monochromator composed of two 0.5 m grating spectrometers and detected on a germanium photodetector using lock-in detection. PL wafer images were obtained by illuminating the entire wafer area at 10 K with a defocused 532 nm laser beam and collecting the image on a commercial video camera. Laser light and wetting-layer PL were excluded from the image by placing a red filter and a 895 nm long pass filter in front of the camera.

Acknowledgment. Support from NSA/ARO and ONR is acknowledged. M.K.Y. is a NRC Research Associate at the Naval Research Laboratory.

REFERENCES AND NOTES

1. Barth, J.; Costantini, G.; Kern, K. Engineering Atomic and Molecular Nanostructures at Surfaces. *Nature* **2005**, *437*, 671–679.
2. Wang, L.; Rastelli, A.; Kiravittaya, S.; Benyoucef, M.; Schmidt, O. G. Self-Assembled Quantum Dot Molecules. *Adv. Mater.* **2009**, *21*, 2601–2618.
3. Krenner, H. J.; Sabathil, M.; Clark, E. C.; Kress, A.; Schuh, D.; Bichler, M.; Abstreiter, G.; Finley, J. J. Direct Observation of Controlled Coupling in an Individual Quantum Dot Molecule. *Phys. Rev. Lett.* **2005**, *94*, 057402.
4. Stinaff, E.; Scheibner, M.; Bracker, A.; Ponomarev, I.; Korenev, V.; Ware, M.; Doty, M.; Reinecke, T.; Gammon, D. Optical Signatures of Coupled Quantum Dots. *Science* **2006**, *311*, 636–639.
5. Scheibner, M.; Bracker, A. S.; Kim, D.; Gammon, D. Essential Concepts in the Optical Properties of Quantum Dot Molecules. *Solid. State Commun.* **2009**, *149*, 1427–1435.
6. Songmuang, R.; Kiravittaya, S.; Schmidt, O. G. Formation of Lateral Quantum Dot Molecules Around Self-Assembled Nanoholes. *Appl. Phys. Lett.* **2003**, *82*, 2892–2894.
7. Alonso-Gonzalez, P.; Martin-Sanchez, J.; Gonzalez, Y.; Alen, B.; Fuster, D.; Gonzalez, L. Formation of Lateral Low Density In(Ga)As Quantum Dot Pairs in GaAs Nanoholes. *Cryst. Growth Des.* **2009**, *9*, 2525–2528.
8. Heidemeyer, H.; Muller, C.; Schmidt, O. Highly Ordered Arrays of In(Ga)As Quantum Dots on Patterned GaAs(001) Substrates. *J. Cryst. Growth* **2004**, *261*, 444–449.
9. Lee, H.; Johnson, J. A.; He, M. Y.; Speck, J. S.; Petroff, P. M.

Strain-Engineered Self-Assembled Semiconductor Quantum Dot Lattices. *Appl. Phys. Lett.* **2001**, *78*, 105–107.
10. Suraprapapich, S.; Shen, Y.; Odnoblyudov, V.; Fainman, Y.; Panyakeow, S.; Tu, C. Self-Assembled Lateral Bi-quantum-dot Molecule Formation By Gas-Source Molecular Beam Epitaxy. *J. Cryst. Growth* **2007**, *301−302*, 735–739.
11. Mui, D. S. L.; Leonard, D.; Coldren, L. A.; Petroff, P. M. Surface Migration Induced Self-Aligned InAs Islands Grown by Molecular Beam Epitaxy. *Appl. Phys. Lett.* **1995**, *66*, 1620–1622.
12. Williams, R. L.; Aers, G. C.; Poole, P. J.; Lefebvre, J.; Chithrani, D.; Lamontagne, B. Controlling the Self-Assembly of InAs/InP Quantum Dots. *J. Cryst. Growth* **2001**, *223*, 321–331.
13. Zhang, R.; Tsui, R.; Shiralagi, K.; Convey, D.; Goronkin, H. Selective formation and Alignment of InAs Quantum Dots over Mesa Stripes Along the [011] and [001] Directions on GaAs (100) Substrates. *Appl. Phys. Lett.* **1998**, *73*, 505–507.
14. Lee, J. H.; Wang, Z. M.; Strom, N. W.; Mazur, Y. I.; Salamo, G. J. InGaAs Quantum Dot Molecules Around Self-Assembled GaAs Nanomound Templates. *Appl. Phys. Lett.* **2006**, *89*, 202101.
15. Kiravittaya, S.; Rastelli, A.; Schmidt, O. G. Advanced Quantum Dot Configurations. *Rep. Prog. Phys.* **2009**, *72*, 046502.
16. Koguchi, N.; Ishige, K. Growth of GaAs Epitaxial Microcrystals on an S-Terminated GaAs Substrate by Successive Irradiation of Ga and As Molecular-Beams. *Jpn. J. Appl. Phys. Part 1* **1993**, *32*, 2052–2058.
17. Heyn, C.; Stemmann, A.; Schramm, A.; Welsch, H.; Hansen, W.; Nemcsics, A. Regimes of GaAs Quantum Dot Self-Assembly by Droplet Epitaxy. *Phys. Rev. B* **2007**, *76*, 075317.
18. Sablon, K. A.; Lee, J. H.; Wang, Z. M.; Shultz, J. H.; Salamo, G. J. Configuration Control of Quantum Dot Molecules by Droplet Epitaxy. *Appl. Phys. Lett.* **2008**, *92*, 203106.
19. Heyn, C.; Stemmann, A.; Schramm, A.; Welsch, H.; Hansen, W.; Nemcsics, A. Faceting During GaAs Quantum Dot Self-Assembly by Droplet Epitaxy. *Appl. Phys. Lett.* **2007**, *90*, 203105.
20. Goldstein, L.; Glas, F.; Marzin, J. Y.; Charasse, M. N.; Roux, G. L. Growth By Molecular Beam Epitaxy and Characterization of InAs/GaAs Strained-Layer Superlattices. *Appl. Phys. Lett.* **1985**, *47*, 1099–1101.
21. Xie, Q.; Madhukar, A.; Chen, P.; Kobayashi, N. P. Vertically Self-Organized InAs Quantum Box Islands on GaAs(100). *Phys. Rev. Lett.* **1995**, *75*, 2542–2545.
22. Solomon, G. S.; Trezza, J. A.; Marshall, A. F.; Harris, J. S., Jr. Vertically Aligned and Electronically Coupled Growth Induced InAs Islands in GaAs. *Phys. Rev. Lett.* **1996**, *76*, 952–955.
23. Albert, F.; Stobbe, S.; Schneider, C.; Heindel, T.; Reitzenstein, S.; Höfling, S.; Lodahl, P.; Worschech, L.; Forchel, A. Quantum Efficiency and Oscillator Strength of Site-Controlled InAs Quantum Dots. *Appl. Phys. Lett.* **2010**, *96*, 151102.
24. García, J. M.; Medeiros-Ribeiro, G.; Schmidt, K.; Ngo, T.; Feng, J. L.; Lorke, A.; Kotthaus, J.; Petroff, P. M. Intermixing and Shape Changes During the Formation of InAs Self-Assembled Quantum Dots. *Appl. Phys. Lett.* **1997**, *71*, 2014–2016.
25. Wasilewski, Z. R.; Fafard, S.; McCaffrey, J. P. Size and Shape Engineering of Vertically Stacked Self-Assembled Quantum Dots. *J. Cryst. Growth* **1999**, *201−202*, 1131–1135.